

Research Article

Open Access

Antonio Mario Federico, Osvaldo Bottiglieri, Francesco Cafaro*, Gaetano Elia

Hydraulic Characterization of a Self-Weight Compacted Coal

<https://doi.org/10.2478/sgem-2019-0031>

received May 2, 2019; accepted September 17, 2019.

Abstract: Water infiltration through coal stocks exposed to weather elements represents a key issue for many old mining sites and coal-fired power plants from the environmental point of view, considering the negative impact on human health of the deriving groundwater, soil and air pollution. Within this context, the paper investigates the hydraulic behaviour of a self-weight compacted unsaturated coal mass and its impact on the numerical prediction of infiltration induced by rainfall events. In particular, the work focuses on the experimental investigation carried out at different representative scales, from the grain scale to physical modelling. The material, when starting from uncompacted conditions, seems to be characterized by metastable structure, which tends to collapse under imbibition. In addition, direct numerical predictions of the seepage regime through a partially saturated coal mass have been performed. As the compaction of the coal stock induced by dozers has not been taken into account, the numerical simulations represent a conservative approach for the assessment of chemical pollution hazard associated to water infiltration into a real stockpile under operational conditions.

Keywords: Environmental engineering, seepage, coal stocks, unsaturated soils, porous-media characterisation, mining and environmental issues

1 Introduction

The stocks of coal are crucial areas of coal-fired power plants, in terms of safety, optimization of energy storage and environmental implications (e.g., [1], [2]). Although they are now usually protected from rain and wind by storage structures or more simply by coating with tarpaulins, in many old plants in the world these stocks are still exposed to natural climatic conditions such as rain. This climatic condition could allow the air pollution with fine coal particles, as close to mining areas (e.g., [3]), and leaching processes due to rainwater infiltration through the coal mass. In principle, this last phenomenon could transfer some heavy metals to the soil and groundwater below the coal stocks, unless natural geological or artificial barriers are interposed at the bottom of the stocks. In this respect, when big piles of coal are exposed to rainfall, a reliable numerical simulation of the seepage through the coal mass becomes a crucial aspect of the environmental safety assessment. It could be carried out by adopting a preliminary and simplified approach with no chemo-hydraulic coupling, where the water medium is seen as a vehicle for pollutant migration.

Coal is a hygroscopic and porous natural material, usually found to be saturated with water in situ.^[4] Differently, in a stockpile the coal blocks and grains are not submerged in water. According to Unsworth et al.,^[4] the moisture in particulate coal is within the pore structure of the particles, on external surfaces and within inter-particle voids. Furthermore, coal surfaces are characterized by a combination of hydrophobic and hydrophilic sites.^[5,6] Therefore, the water flow through a coal mass is a complex process requiring experimental investigation at different scales, also adopting a strategy of characterization based on physical modelling,^[7,8] since element testing alone would not give results representative of the entire mass.

It should be noted that coal stockpiles are usually compacted by dozers, under water unsaturated conditions. Coal crushing in the top layers during compaction was observed to be the main cause of the appearance of fine grains (e.g., [9]): the resulting variation in particle size

*Corresponding author: Francesco Cafaro, Department of Civil, Environmental, Land, Building Engineering and Chemistry (DICATECh), Technical University of Bari (Politecnico di Bari), via Orabona 4, 70125 Bari, Italy, E-mail: francesco.cafaro@poliba.it
Antonio Mario Federico, Osvaldo Bottiglieri, Gaetano Elia, Department of Civil, Environmental, Land, Building Engineering and Chemistry (DICATECh), Technical University of Bari (Politecnico di Bari), via Orabona 4, 70125 Bari, Italy

Table 1: Compositional data of the coal (* Proximate Analysis ** Ultimate Analysis)

Determination	Standard/Method	Weight (%)	Note
Moisture in the Analysis Sample*	ISO 11722:1999	11.1	Air Dried Basis
Ash Content*	ISO 1171:2010 (E)	5.8	As Received Basis
Volatile Matter*	ISO 562:2010 (E)	37.4	As Received Basis
Fixed Carbon*	By calculation	42.3	As Received Basis
Carbon**	ASTM D 5373-08	65.7	Air Dried Basis
Hydrogen**	ASTM D 5373-08	4.4	Air Dried Basis
Nitrogen**	ASTM D 5373-08	1.3	Air Dried Basis
Sulphur**	ASTM D 4239-10	0.8	Air Dried Basis
Oxygen**	By calculation	10.7	Air Dried Basis

distribution leads to the reduction of porosity of the top strata, with a consequent decrease of the material permeability. Within this context, the implementation in the seepage modelling of a loose (i.e., uncompacted) coal mass represents a conservative approach to define an ‘upper limit’ of the flow rate and, therefore, to increase the safety in the assessment of groundwater chemical contamination hazard.

The approach followed in this research looks at the coal mass as an unsaturated compacted granular soil, thus allowing to adopt the framework developed for non-cohesive partially saturated soils. In this respect, a numerical prediction of a seepage process through an unsaturated geo-material needs the knowledge of its hydraulic functions, that is, the water retention curve (WRC) and the hydraulic conductivity function $k(s)$, for example using the formulations proposed by van Genuchten^[10] and Mualem.^[11] This allows to solve the Richards’ equation^[12] and, thus, to predict the water discharge at the bottom of the stockpile, once the geometrical model and the hydraulic boundary conditions are fully defined. The water retention curve of soils depends on their porosity.^[13,14,15,16,17,18] For fine-grained deformable soils, the retention curve can be controlled by the material stiffness too,^[19] thus requiring a fully coupled hydro-mechanical modelling.^[20] However, in the case of a coal mass, this aspect can be reasonably neglected due to the relatively high stiffness of the grain assembly, as discussed in the next section.

In this work, based on the abovementioned perspective, the hydraulic properties of a self-weight compacted Indonesian coal mass have been deduced by physical modelling, through an inverse numerical analysis of the transient seepage associated to a controlled infiltration process. Further aim of the work was to investigate the

performance as ‘hydraulic barrier’ of an ideal stockpile made of the studied coal, by using the back-analysed hydraulic functions in a boundary value problem.

The following sections present a number of experimental investigations, consisting of: i) stages of water imbibition of coal samples at the element volume scale and ii) one-dimensional hydraulic physical modelling of a coal stockpile, together with the inverse analysis based on the suction data monitored in the physical model. Using the hydraulic functions obtained by numerical optimization of the simulation of flow through the partially saturated coal mass, the results of direct numerical predictions of the seepage regime induced by rainfall of different intensities in a real scale coal stockpile are finally shown and discussed.

2 Coal composition and assessment of retention behaviour at element volume scale

The water retention properties of coals are a function of their carbon content and rank related to the coalification process.^[21] According to Tamy et al.,^[5] as the coal rank increases, the coal becomes more hydrophobic, up to a carbon content of about 90%, whereas beyond this value, the hydrophobicity decreases. Moreover, higher rank coals seem to be less prone to swelling under wetting than lower rank ones.^[22] Therefore, the hydraulic behaviour of this kind of material must be seen in the light of its composition. Some compositional data of the studied coal are reported in Table 1, whereas Figure 1 shows the particle size distribution curves of the coal, obtained through standard dry sieving analysis. Although derived

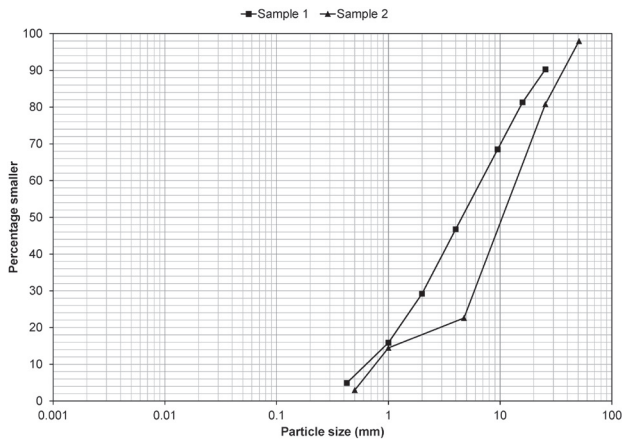


Figure 1: Particle size distribution of two coal samples.



Figure 2: Block of Indonesian Coal subjected to swelling/shrinkage test.

for two different samples, the curves shown in Figure 1 are substantially similar. This coarse material is well-graded, with coefficients of uniformity equal to 10.5 and 13.7, thus indicating the presence of a wide range of particle sizes, as a probable effect of high crushability under static and dynamic loads, which can potentially lead to a significant reduction of its porosity.

As shown in Table 1, the carbon content of the coal is about 66% in weight. The coal has a gross calorific value of 6160 kcal/kg, consistently. The specific gravity (G_s) of the coal disintegrated into powder, that is, the ratio of the solid particles' unit weight (γ_s) to the water unit weight (γ_w), was found to be equal to 1.37, using the procedure proposed by Federico et al.^[23] The hygroscopic water content of the material ranges between 6 and 14 %, as measured on individual fragments. This range seems to be consistent with the carbon content, if compared to the data from Fityus and Li,^[21] regarding Permian bituminous coals of low to medium rank, which indicate that the 'intrinsic' water content is higher for lower carbon content.

To understand the interaction between solid phase and water phase at the 'grain' scale, a preliminary investigation stage has concerned the swell/shrinkage ability and the retention capacity of single blocks of coal, representing 'grains' at the stockpile scale. The block shown in Figure 2 was wetted, starting from a hygroscopic water content, by prolonged submersion in distilled water, and measures of both weight and volume have been taken for 7 days. The measurement of volume was made by weighing the mercury displaced by the block when submerged in it. No significant swelling was observed and only a very slight increase of the total weight of the block was detected, thus demonstrating that the intra-particle porosity of this coal does not tend to retain water strongly. The block has then been dried in oven at 105°C for one day and the final volume was measured: the shrinkage during drying was less than 1.9% volumetric strain. Therefore, given the stiffness of the coal blocks and fragments, the change in overall porosity of the physical model described in the following section will be fundamentally attributed to variation of the inter-particle porosity, as a result of reorganization of the granular packing, where the grains are treated as 'nonporous'. In this respect, the dry unit weight of the individual coal blocks and fragments, which is about 12 kN/m³, will be assumed to have the meaning of solid unit weight at the grain scale. From this point on, a 'macro-scale specific gravity' G_s^* will be introduced when referring to a coal mass. Namely, a value of 1.2 for this parameter will be adopted. The difference between G_s and G_s^* is consistent with data from literature.^[24]

A measurement of suction was performed on a coal block of about 200 cm³ and with a water content close to 6%, using the filter paper technique.^[25] A Whatman (grade 42) filter paper was kept in contact with the coal block for 9 days. At the end of the equalization period, a value of the matrix suction equal to approximately 700 kPa was obtained using the calibration procedure proposed by Chandler et al.^[26] In the light of the imbibition test previously mentioned, this relatively high suction value could be related to the ability of the coal blocks to retain water on the external surface, more than within the overall micro-porosity of the material, that is, its intra-particle porosity.

To explore the water retention potential due to the macro-porosity of the coal, that is, its inter-particle porosity, preliminary tests on representative cylindrical samples have been carried out. They consisted in controlled wetting stages of different samples of coal by introducing an assigned volume of water, corresponding to a rain of given intensity and duration. The samples have been set in a PVC cylindrical cell of height and

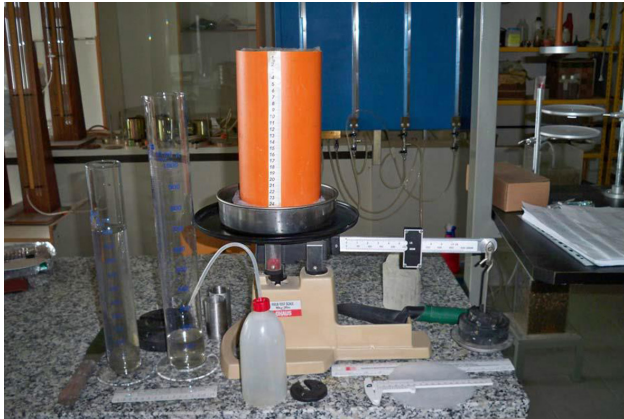


Figure 3: PVC cylindrical cell for the preliminary evaluation of the water retention potential of the coal.

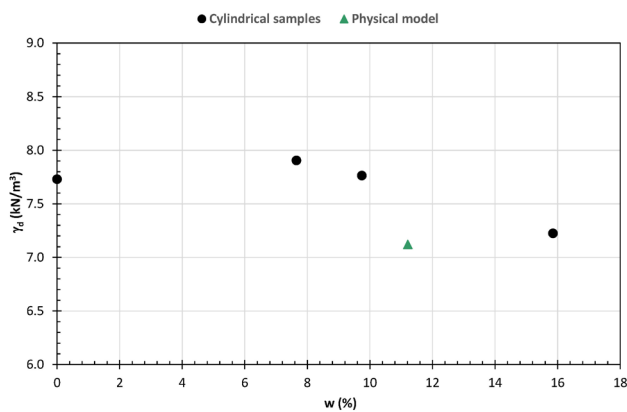


Figure 4: Dry unit weights of coal cylindrical samples and physical model

inner diameter equal to 0.25 m and 0.135 m, respectively (Figure 3). The cell ensures a free drainage condition at the bottom and, furthermore, it was placed on a weigh-beam inside a container that collects the water that flows out from the base. This configuration has allowed to perform a hydraulic balance between the water volumes added from the top surface of the sample, retained by the coal and drained out through the bottom. The coal samples have been prepared by gradually filling the cell up to a height of 0.24 m and allowing a compaction by self-weight only. They have been, then, wetted by adding an amount of water corresponding to a one-day rainfall of 94 mm. Table 2a shows the initial physical-volumetric state reached by the coal samples, where w_0 is the initial gravimetric water content, γ and γ_d are the total and dry unit weight respectively, e_0 is the initial void ratio, S_r is the degree of saturation and θ_w is the volumetric water content, equal to $S_r \times n$, where n is the porosity. Figure 4 shows the irrelevant effect of the initial water content on the coal dry unit

weight after self-weight compaction. The test was iterated four times, starting from different water contents of the sample before each wetting stage.

The wetting stages consisted of the addition of the above-defined volume of water through five steps of 12 minutes each, thus confining the one-day reference rain in one hour. The resulting final states of the samples are summarized in Table 2b. The results of the hydraulic balance point out an overall increase of the volumetric water content due to the imbibition stages, which is a consequence of a not negligible water retention capacity of the coal mass.

The measurement of the final height of the samples has allowed to deduce that each specimen has experienced a volumetric collapse. The principle of effective stress^[27] cannot explain this behaviour that naturally occurs during the imbibition of some water unsaturated soils, defined as ‘collapsible’, and is then more appropriate to use the concepts of unsaturated soil mechanics to explain such volumetric collapse.^[28,29,30,31] Qian and Lin^[32] recognized a category of soils (generally non-cohesive), which collapse upon wetting under a total pressure equal to their overburden. This could justify a wetting collapse for coals even at low confining stress, as measured for the coal samples investigated in this study.

3 Experimental investigation of the hydraulic functions

The experimental set up for the measurement of suction during a one-dimensional infiltration process into a physical model of a coal mass is presented here. The back-analysis of the data measured at prototype scale has allowed to calibrate the parameters of the hydraulic functions characterizing the material, accounting for the change of porosity induced by the wetting collapse of the partially saturated coal column. The geometrical features and the physical-volumetric state of the prototype model in its initial condition are discussed first; subsequently, the inverse analysis of the measured suction data is presented.

3.1 Physical modelling of one-dimensional infiltration

Figure 5 shows the prototype manufactured for the physical modelling. It has a regular prismatic shape with a square section, with height of 114 cm and base of 50

Table 2: Physical-volumetric parameters of the coal cylindrical samples: a) at initial state; b) after imbibition

a)

Sample	w_0	γ_0 (kN/m ³)	G_s^*	γ_d (kN/m ³)	e_0	S_r	θ	drying procedure / time (day)
1	15.9%	8.4	1.2	7.2	0.63	30%	0.12	hygroscopic / -
3	9.7%	8.5	1.2	7.8	0.52	23%	0.08	free drying / 2
2	7.7%	8.5	1.2	7.9	0.49	19%	0.06	free drying / 4
4	0.0%	7.7	1.2	7.7	0.52	0%	0.00	oven drying at 105°C / 2

b)

Sample	w	γ (kN/m ³)	G_s^*	γ_d (kN/m ³)	e	S_r	θ
1	27.5%	9.7	1.2	7.6	0.54	61%	0.21
3	26.3%	10.7	1.2	8.5	0.39	81%	0.23
2	26.8%	10.5	1.2	8.2	0.43	75%	0.23
4	27.7%	10.3	1.2	8.1	0.46	72%	0.23



Figure 5: a) View of coal during drying at room temperature; b) phase of prototype filling

cm. One of the vertical side panels is made of Plexiglass to allow for visual inspection of the advancement of the wet front. The prototype model is provided at the bottom with a hopper and a metallic grid, to collect the efflux flow and, at the same time, retain the material. A filtering sheet was also placed on the metallic grid. The model has three housings along the central vertical on one of the side panel for the insertion of mini-tensiometers (provided by Soilmoisture Equipment) used for the continuous logging of the matrix suction values (Figures 6a and 6b). Details of the mini-tensiometers are shown in Figure 6c, where the porous tip allowing for suction measurements is clearly visible.

The choice of a physical modelling for the determination of the hydraulic properties of the material

comes from the following considerations: i) the particle size of the coal implies that a small laboratory specimen is not really representative of the overall behaviour of the stockpile; ii) the direct experimental evaluation of the hydraulic conductivity in partially saturated conditions is complex and somehow unreliable (e.g., [33], [34]). For these reasons, the hydraulic conductivity, in conjunction with the retention curve, can be deduced by means of an inverse numerical analysis of an infiltration process with known initial conditions of partial saturation (e.g., [35], [7], [36], [8], [37]).

The physical model was prepared by filling the box with coal, previously left to dry at room temperature (Figure 5a) and then poured in successive layers (Figure 5b) to create the initial fabric of a self-weight compacted

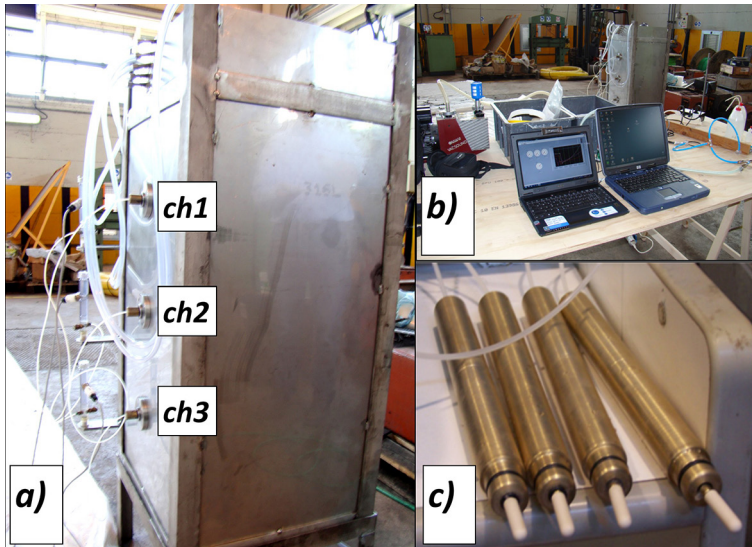


Figure 6: a) Location of the mini-tensiometers; b) continuous data logging system; c) details of the mini-tensiometers

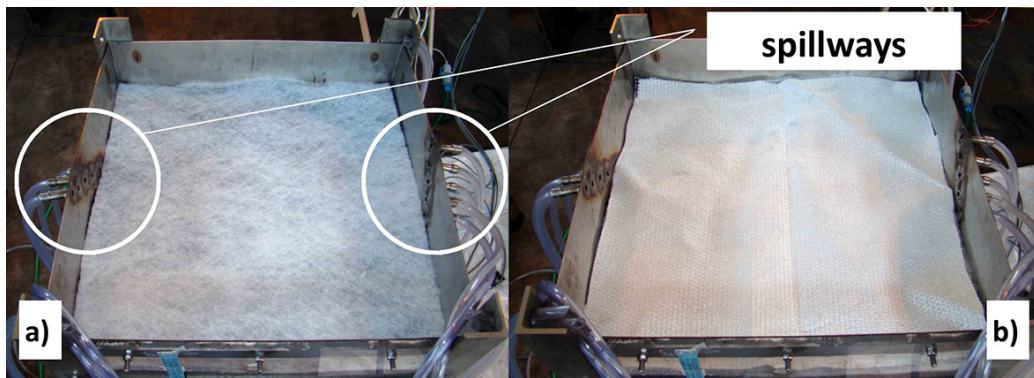


Figure 7: Spillways detail and filtering sheets: a) first layer; b) second layer

material. The coal of each layer, before being poured in the model, was weighed and its gravimetric water content (w_0) was determined. The data collected for each layer and the measurements of the column height (H) have allowed to deduce the wet and dry total weights of the physical model and, on average, its physical-volumetric state in the initial condition reported in Table 3a, where W_0 and W_d are the initial and dry weights of the coal mass, respectively. It should be noted that the dry unit weight of the coal in the physical model is similar to that of the cylindrical samples discussed before, as shown in Figure 4.

Once the box was filled with coal, the three mini-tensiometers were inserted in their housings (as shown in Figure 6a), being sure that the necessary de-aeration of the circuits^[38] was carried out. The mini-tensiometers were connected to three different channels of the logging system, named, from top to bottom, ch1, ch2 and ch3. They were left to equalize for about 24 hours, recording

suction values equal, on average, to 60 kPa (Table 4a). The small discrepancy between the values suggests a good homogeneity of the prototype model in terms of initial porosity and humidity.

A drainage filter, obtained by overlapping two different sheets of synthetic fabric with relatively high water permeability, was placed on the top face of the coal model (as shown in Figure 7), in order to avoid loss of material at the upper surface due to water splashes at the start of the imbibition process. Five pairs of spillways at different heights allow to assign five different conditions in terms of constant hydraulic head to the top boundary of the prototype. Moreover, the previously mentioned metallic grid guarantees free drainage boundary condition at the bottom of the model.

For the first imbibition of the prototype, hydraulic head of 10 cm was created by opening the appropriate pair of spillways. In the short transitory phase during which

Table 3: Physical-volumetric parameters of the coal in the prototype model: a) at initial state; b) after volumetric collapse

a)					
w_0	W_0 (N)	W_d (N)	H (m)	V (m ³)	G_s^*
11.21%	1984	1784	1.002	0.2505	1.20
γ (kN/m ³)	γ_d (kN/m ³)	e	n	S_r	θ
7.92	7.12	0.65	0.39	20.61%	0.081
b)					
w	W (N)	W _d (N)	H (m)	V (m ³)	G _s [*]
39.87%	2491	1781	0.895	0.2238	1.20
γ (kN/m ³)	γ_d (kN/m ³)	e	n	S_r	θ
11.13	7.96	0.48	0.32	100%	0.324

Table 4: Matric suction values measured along the central vertical of the prototype model: a) at initial state; b) during the drying phase

a)		
ch1	ch2	ch3
(kPa)	(kPa)	(kPa)
61.9	56.3	65.1
b)		
<i>After 7 days of drying at room temperature</i>		
ch1	ch2	ch3
(kPa)	(kPa)	(kPa)
2.5	2.5	2.5
<i>After 14 days of drying at room temperature</i>		
ch1	ch2	ch3
(kPa)	(kPa)	(kPa)
15.0	15.0	15.0

the hydraulic head was brought to the desired level, the infiltration process was temporarily prevented by covering the top face of the coal pile with an impermeable sheet, then quickly removed to trigger the infiltration process.

As mentioned before, the coal was deposited in the physical model under its own weight, at a relatively low water content. This has involved a fabric for the coal mass in the model that could be defined as ‘virgin’, characterized by a high porosity (with an initial void ratio of 0.65, Table 3a). This open fabric would make the material skeleton prone to reorganization toward a more dense packing. Indeed, the first infiltration test, which allowed to infer the retention and hydraulic conductivity

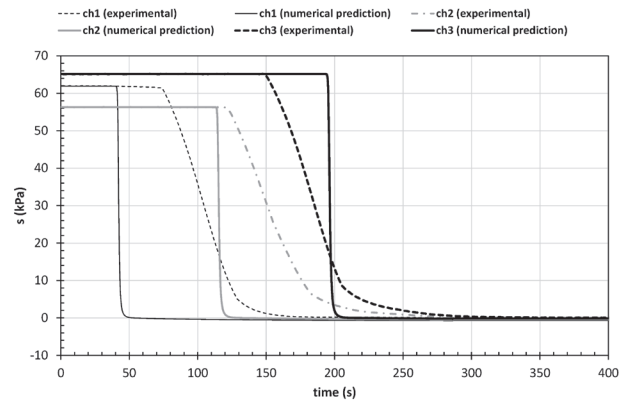


Figure 8: First imbibition phase: experimental data and corresponding numerical results

functions of the material in its virgin state, has also caused further compaction. In fact, the constant hydraulic head of about 10 cm applied to the top boundary of the model has caused two combined phenomena: the washing of the coal itself, due to the downward movement of the powder carried by the infiltrated water, and a significant reduction of the void ratio, from 0.65 to 0.48 (as reported in Table 3b). The second process can be seen as a volumetric collapse under imbibition of a partially saturated material, a phenomenon widely found in the literature, as already discussed in the second section.

Figure 8 shows the time histories of the matric suction measured through the continuous logging system in the three observation points during the first infiltration test. The suction reduces to zero at the three tensiometers at different times; this offset is clearly due to the progressive arrival of the wet front at the three measurement points. Starting from this new volumetric state, the physical model was left at room temperature and then subjected to evaporation for about two weeks. At the end of this period, during which the suction values (Table 4b) and the volumetric states (Table 5) were closely monitored, a second infiltration test was carried out, this time imposing at the top a constant flow rate (equal to $7.32 \cdot 10^{-2}$ mm/s) as a boundary condition.

3.2 Inverse analysis of one-dimensional infiltration

In the hypothesis of one-dimensional conditions (i.e., assuming that the flow is not affected by end effects), the inverse numerical analysis of the two infiltration tests was carried out using Hydrus-1D.^[39] This is a software for the simulation of one-dimensional water flow in partially-

Table 5: Physical-volumetric state of the coal in the prototype model during the drying phases

<i>After 7 days of drying at room temperature</i>					
w	W (N)	W _d (N)	H (m)	V (m ³)	G _s [*]
17.70%	2096	1781	0.895	0.2238	1.20
γ (kN/m ³)	γ _d (kN/m ³)	e	n	S _r	θ
9.37	7.96	0.48	0.32	44.39%	0.144
<i>After 14 days of drying at room temperature</i>					
w	W (N)	W _d (N)	H (m)	V (m ³)	G _s [*]
16.73%	2082	1781	0.895	0.2238	1.20
γ (kN/m ³)	γ _d (kN/m ³)	e	n	S _r	θ
9.31	7.96	0.48	0.32	41.97%	0.136

saturated media, that numerically solves, using a standard Galerkin-type linear finite element scheme, the Richards' equation. Hydrus-1D also includes a Marquardt-Levenberg type parameter optimization algorithm for the inverse estimation of soil hydraulic parameters from measured transient or steady-state flow. The finite element model is composed by 101 nodes. The formulation proposed by van Genuchten^[10] in conjunction with the statistical model on the porosimetric distribution developed by Mualem^[11] was adopted in the simulations:

$$\begin{cases} \theta(s) = \theta_r + \frac{\theta_0 - \theta_r}{\left[1 + (\alpha s)^n\right]^m} & s > 0 \\ \theta(s) = \theta_0 & s = 0 \end{cases} \quad (1)$$

$$\begin{cases} k(s) = k_s \Theta^l \left[1 - (1 - \Theta^{1/m})^m\right]^2 & s > 0 \\ k(s) = k_s & s \leq 0 \end{cases} \quad (2)$$

with:

$$\Theta = \frac{\theta - \theta_r}{\theta_0 - \theta_r} \quad (3)$$

where s is the suction, θ_r and θ_0 are the residual and the saturated volumetric water content, respectively, k_s is the saturated hydraulic conductivity, while α , m , n' and l represent the interpolation parameters (with $m = 1 - 1/n'$).

The inverse analyses of the two imbibition processes and the interpretation of the drying stage have been aimed at inferring the parameters of the coal hydraulic retention

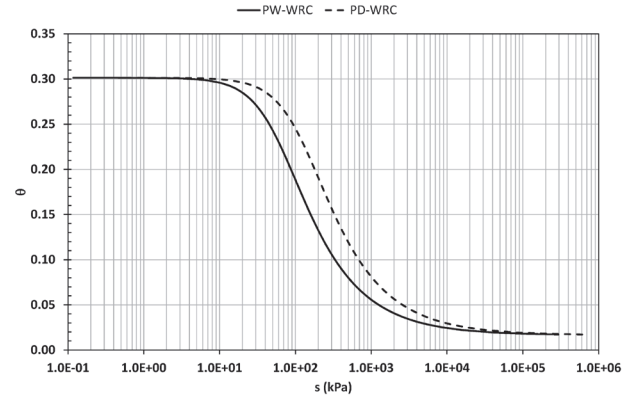


Figure 9: Water retention curves

and conductivity functions according to the model formalized by the set of Equations (1–3).

The time histories of suction predicted by the software during the first imbibition of the physical model are presented in Figure 8, together with the actual recorded data previously shown. The numerical predictions are in good agreement with the experimental data. The results have been obtained through an iterative optimization process, once the range of the six unknown parameters (i.e., θ_r , θ_0 , α , n' , k_s and l) was defined on the basis of the initial physical-volumetric characterization of the coal (Table 2a) and considering the data available in the literature. Table 6a reports the parameters resulting from this first inverse analysis, characterized by a correlation coefficient r^2 equal to 0.8. Figure 9 and Figure 10 show the corresponding retention curve (named as PW-WRC) and conductivity function (indicated with PW-k(s)) obtained for the first infiltration test, respectively.

The first wetting of the coal mass in the prototype, in addition to induce a volumetric collapse leading to a higher degree of compaction (see Table 2b) and a more stable fabric than the initial one, has allowed to confine within a range some of the parameters controlling the shape of the retention curve during wetting. The same range was adopted for the drying branch of the WRC in the numerical simulations. Although the drying and wetting retention curves differ due to hysteresis phenomena, many authors (e.g., [40], [35]) have noted that, for practical purposes, it can be assumed that they have in common the slope of the transition branch, and therefore the parameter n' , and the extreme volumetric water contents θ_r and θ_0 . On the contrary, the threshold value of suction marking the transition from partially saturated to almost fully saturated conditions is different for the two paths. This suction, linked to the parameter α , is generally

Table 6: Hydraulic function parameters: a) at the first infiltration test; b) at the second infiltration test

a)						
θ_r	θ_0	α	$a=1/\alpha$	n'	k_s	l
		(kPa) ⁻¹	(kPa)		(m/s)	
0.0165	0.3014	1.670	0.598	1.703	8.0E-04	1
b)						
θ_r	θ_0	α	$a=1/\alpha$	n'	k_s	l
		(kPa) ⁻¹	(kPa)		(m/s)	
0.0165	0.3014	0.812	1.231	1.703	1.0E-05	1

Table 7: WRC parameters for the drying phase following the first imbibition stage

θ_r	θ_0	α	$a=1/\alpha$	n'
		(kPa) ⁻¹	(kPa)	
0.0165	0.3014	0.812	1.231	1.703

known in the literature as Air Entry Value (AEV), although this notation is more correct if referring to desaturation processes. In the light of the above-mentioned, the drying retention curve of the coal was already partly defined, since the parameters θ_r , θ_0 and n' have been already determined during the first inverse analysis. Therefore, the parameter still unknown, that is, α (which is function of the AEV during drying), was deduced by non-linear regression, according to the van Genuchten formulation of the retention function and the drying conditions measured in terms of s and θ reported in Tables 4b and 5, respectively. The value of the parameter α resulting from the non-linear regression, carried out with the software RETC,^[41] is shown in Table 7. The resulting drying WRC is shown in Figure 9 (named as PD-WRC).

As already said, the second wetting stage of the coal prototype was carried out 14 days after the first infiltration test. The resulting degree of saturation reported in Table 5 is still quite high compared to its initial value (see Table 3a). When the volumetric water content is high compared to the residual value θ_r and, therefore, close to the ‘knee’ defined by the AEV, the state of the material in humidification follows the retention curve towards θ_0 along a small branch. An inverse analysis of the data recorded during drying, to infer further information on the shape factors of the WRC, would therefore be of little significance. On the contrary, an inverse analysis is more useful if aimed at back-calculating the saturated permeability k_s , which

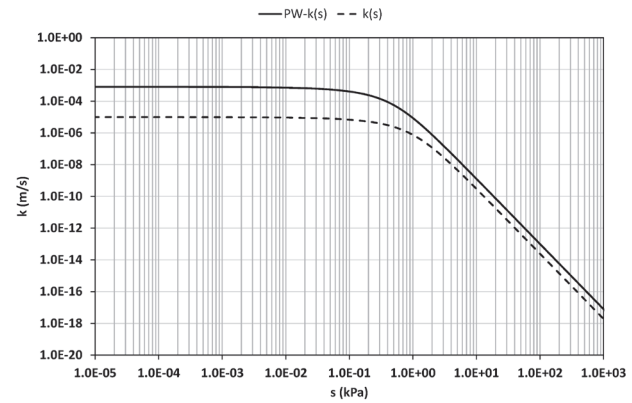


Figure 10: Conductivity functions

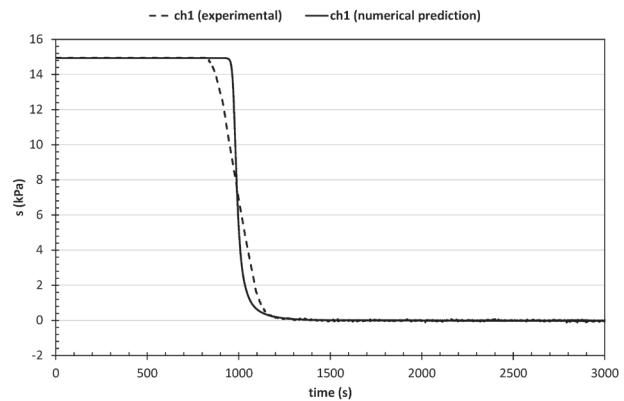


Figure 11: Comparison between measured and predicted variation of suction with time at ch1

is strongly affected by the compaction caused by the first imbibition. Also, in this case, an iterative optimization process was carried out with Hydrus-1D. The resulting k_s value is reported in Table 6b and is about two orders of magnitude smaller than that determined by the first inverse analysis (see Table 6a). Figure 10 shows the corresponding optimized conductivity function (indicated as $k(s)$).

Figure 11 shows the comparison between the experimental variation of suction with time recorded at ch1 in the prototype and the numerical prediction achieved implementing the retention curve deduced in drying, which from now on will be assumed as ‘unique’ and valid also for the re-humidification branch, and the new conductivity function, that is, updated with the saturated permeability obtained from the optimization process described above. For this new prediction, the correlation coefficient r^2 is equal to 0.99.

Finally, retention and conductivity parameters of the studied coal are compared in Table 8 with the values measured for other kinds of granular materials.^[8, 42, 43] It

Table 8: Hydraulic properties of the Indonesian coal in comparison to other granular materials

<i>Material</i>	<i>a (kPa)</i>	<i>k_s (m/s)</i>
Indonesian Coal – virgin state (<i>present study</i>)	0.60	8.0E-4
Indonesian Coal – after collapse (<i>present study</i>)	1.23	1.0E-5
Silty Clayey Sand (<i>Cafaro et al. 2008</i>)	0.63	1.58E-6
Pervious Concrete – different mixtures (<i>Marzulli et al. 2018</i>)	3.07 1.56	2E-4 5E-3
Sand (<i>Lu and Likos 2004</i>)	10	3E-4

should be underlined, however, that the differences in the parameter values can result from both the variability of the geomaterials and the experimental and numerical techniques adopted for their determination.

4 Hydraulic performance of an ideal stockpile after primary wetting collapse

In order to investigate the effect of coal hydraulic properties on the rate of rainwater infiltration into a real scale stockpile, a numerical analysis was performed considering different scenarios, that is, adopting the retention and conductivity functions deduced in the first part of the work and changing the initial suction within the stockpile and the intensity of the rainfall. Therefore, the impact of the aforementioned hydraulic functions on the direct numerical prediction of the seepage regime induced by the rainfall in a stockpile was assessed. In particular, a coal mass characterized by a degree of compaction similar to that obtained in the physical model after the volumetric collapse caused by the first imbibition (i.e., primary wetting collapse) was considered. To isolate the effect of compaction resulting from wetting collapse, no mechanical compaction of the stockpile induced by dozers was taken into account.

The seepage through a coal deposit with an overall thickness of 7 m was simulated using Hydrus-1D, assuming a one-dimensional model, composed by 71 nodes, with a free drainage boundary condition at the bottom. The initial condition of the coal deposit was changed accounting for two possible scenarios: one corresponding to a dry

material, with an initial suction of 60 kPa, and the other one representing an initially wet deposit, with a suction equal to 30 kPa. The suction was assumed to be constant with depth within the stockpile. This assumption implies: a) stress state at static equilibrium; b) absence of capillary rises related to a water table beneath; c) no rain or other humidity contribution from the atmosphere within the time lapse needed to equalize the initial suction.

The investigation has also considered two different hydraulic boundary conditions at the top of the model, that is, two pluviometric input scenarios: in one case, an extreme one day rainfall event, with an inflow rate (q) equal to 10 cm/day, was implemented; while in the other case, a constant rainfall, with an intensity of 1.9 mm/day calculated on the basis of 700 mm of water accumulated over one year, was applied.

The results obtained in terms of evolution over one year of the suction profiles within the stockpile are reported in Figure 12 (a, b, c, d). In particular, the profiles predicted after 12 months from the start of the rainfall showed that the wet front never reached the base of the deposit, with the exception of the case (shown in Figure 12d) of a medium intensity rain (i.e., constant rain applied over one year) acting on a stockpile with an initial suction equal to 30 kPa, that is, to a deposit already wet at the beginning of the rainfall. In this specific case, and only after one year from the beginning of the rain, a very low flow rate equal to 0.07 l/day per square meter of surface can be detected at the bottom of the stockpile. In all other cases, the depth of penetration of the wet front after one year varies between 2 and 6 meters from the top surface. In none of the cases, the suction reaches a null value during the period of time investigated.

5 Conclusions

The hydraulic properties of an Indonesian fossil coal was deduced, in terms of both water retention curve and hydraulic conductivity function, with the experimental multiscale investigation outlined in this work, starting from condition of ‘virgin’ compaction (i.e., initial fabric only due to self-weight deposition). It was found that the material is susceptible to a significant reduction of intergranular porosity correlated with the first imbibition. In particular, the saturated permeability measured by inverse numerical analysis of an infiltration through physical model was seen to decrease of about two orders of magnitude. Accounting for the effect of this ‘primary wetting collapse’ on the saturated hydraulic conductivity,

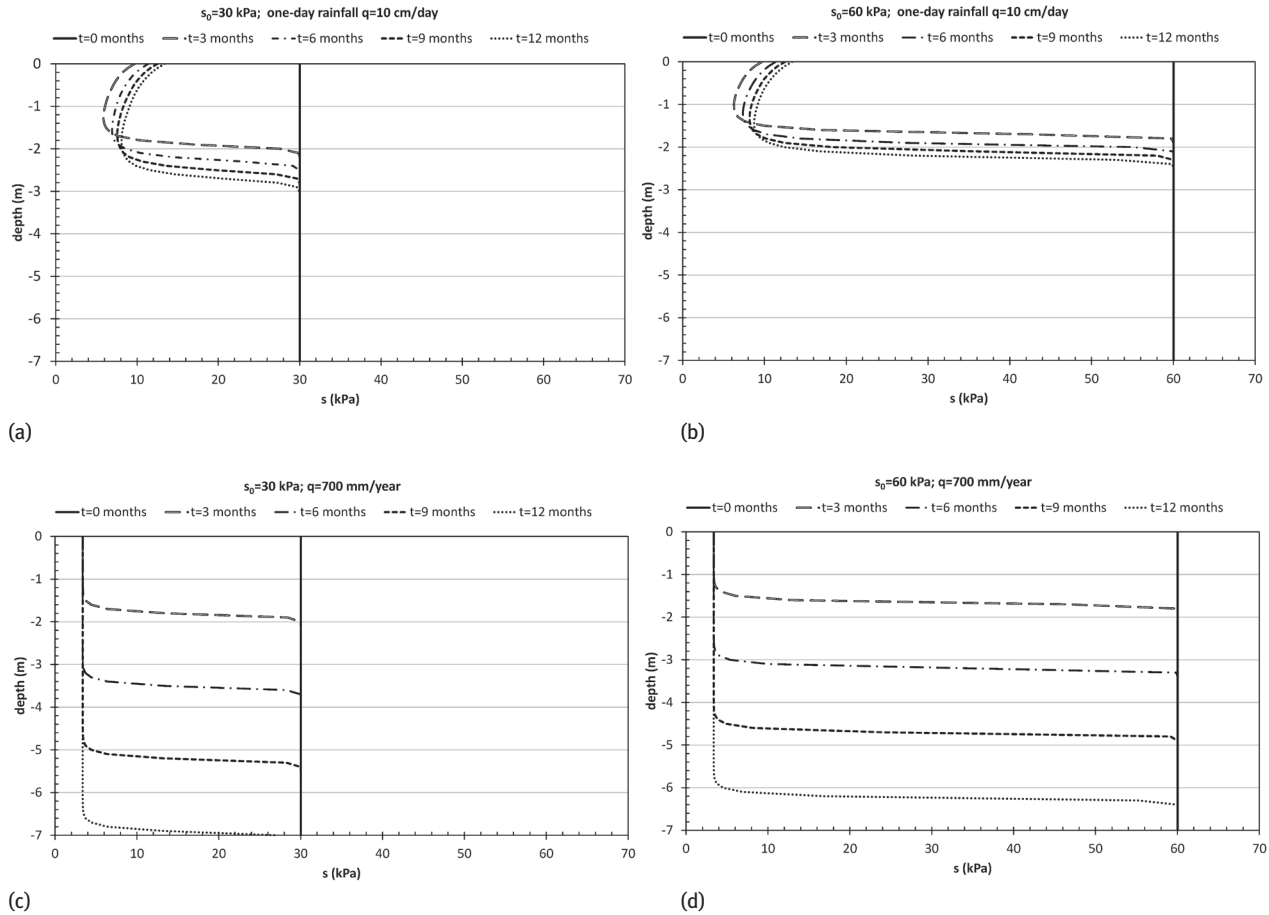


Figure 12: Predicted infiltration due to: (a) an extreme rainfall event through an initially wet stockpile; (b) an extreme rainfall event through an initially dry stockpile; (c) a constant rainfall through an initially wet stockpile; (d) a constant rainfall through an initially dry stockpile.

the numerical simulation of the seepage induced by rainfall in a 7 m thick ideal stockpile with different initial humidity showed that the water flow was not able to reach the bottom free draining section of the coal deposit, except for the case of an initial suction of 30 kPa with constant rainfall of medium intensity and only after almost one year since the start of the rain. In this case, anyway, the calculated flow rates were extremely low. Since the hydraulic conductivity function seems to affect the numerical predictions more than the retention curve, it should be underlined that the saturated permeability used in the simulations (i.e. $k_s = 10^{-5}$ m/s) was plausibly much higher than that of a coal stockpile in situ.

Finally, it must be considered that the granulometric sorting of the investigated coal was relatively high and made the material prone to be highly densified by the static action of a dozer. In addition, the progressive migration of the coal powder over time towards the bottom of the stockpile, especially due to heavy rainfalls, will probably

clog its original porosity, at least partially, making the stock of coal heterogeneous and characterized by a bottom layer with further reduced permeability. Moreover, the evaporation of water from a stockpile will actually subtract an amount of the rain that has been, instead, allowed to infiltrate in the coal deposit in the presented simulations. On the basis of these considerations, it can be argued that the hydraulic behaviour of a compacted coal stockpile under normal operational conditions will be characterized, in the presence of rain, by lower infiltration rates than those calculated in this study. Therefore, the hydraulic characterization undertaken in this work represents an ‘upper limit’ approach for the assessment of the chemical pollution hazard associated to the water infiltration into a real coal stockpile and its foundation soil. Starting from the present study, it can be recommended to implement in the calculation a chemo-hydraulic coupling in order to better predict the transport of pollutants through the coal mass.

Notation List

α, m, n', l : van Genuchten fitting parameters

e_o : initial void ratio

γ : total unit weight

γ_d : dry unit weight

k_s : saturated hydraulic conductivity

θ, θ_w : volumetric water content

n : porosity

G_s : specific gravity

G_s^* : macro-scale specific gravity

s : suction

S_r : degree of saturation

w_o : initial gravimetric water content

W : weight

References

- [1] WWF (2007) Dirty Thirty - Ranking of the most polluting power stations in Europe. WWF European Policy Office.
- [2] European Environmental Agency (2011) Revealing the costs of air pollution from industrial facilities in Europe. EEA Technical Report No. 15/2011.
- [3] Pandey B., Agrawal M., Singh S. (2014) Coal mining activities change plant community structure due to air pollution and soil degradation. *Ecotoxicology* (DOI 10.1007/s10646-014-1289-4).
- [4] Unsworth J.F., Fowler C.S., Heard N.A., Weldon V.L., McBrierty V.J. (1988) Moisture in coal 1. Differentiation between forms of moisture by NMR and microwave attenuation techniques. *Fuel*, 67:1111–1119.
- [5] Tamy G., Prudich M., Savage R., Williams R. (1988) Free energy changes and hydrogen bonding in the wetting of coals. *Energy and Fuels*, 2:787–793.
- [6] Wang N., Sasaki M., Yoshida T., Kotanigawa T. (1998) Estimation of coal hydrophilicity by flow microcalorimetry. *Colloids and Surfaces A: Physicochemical and Engineering Aspects*, 135:11–18.
- [7] Kodesová R. (2003) Determination of hydraulic properties of unsaturated soil via inverse modeling. Lecture given at the College on Soil Physics, Trieste, 3–21 March 2003.
- [8] Cafaro F., Hoffmann C., Cotecchia F., Buscemi A., Bottiglieri O., Tarantino A. (2008) Modellazione del comportamento idraulico di terreni parzialmente saturi a grana media e grossa. *Rivista Italiana di Geotecnica*, 3:54–72 (in Italian).
- [9] Ma D., Rezania M., Yu H-S., Bai H-B. (2017) Variations of hydraulic properties of granular sandstones during water inrush: Effect of small particle migration. *Engineering Geology*, 217:61–70.
- [10] van Genuchten M.T. (1980) A closed form equation for predicting the hydraulic conductivity of unsaturated soils. *Soil Science Society of America Journal*, 44:892–898.
- [11] Mualem Y. (1976) A new model for predicting the hydraulic conductivity of unsaturated porous media. *Water Resources Research*, 12:513–522.
- [12] Richards L.A. (1931) Capillary conduction of liquids through porous media. *Physics*, 1:318–333.
- [13] Vanapalli S.K., Fredlund D.G., Pufahl D.E. (1999) The influence of soil structure and stress history on the soil-water characteristics of a compacted till. *Géotechnique*, 49:143–159.
- [14] Fredlund M.D., Fredlund D.G., Wilson G.W. (2000) Estimation of volume change functions for unsaturated soils. In Rahardjo H., Toll D.G., Leong E.C. (Eds), *Unsaturated Soil for Asia*, 663–668.
- [15] Kawai K., Kato S., Karube D. (2000) The model of water retention curve considering effects of void ratio. In Rahardjo H., Toll D.G., Leong E.C. (Eds), *Unsaturated Soil for Asia*, 329–334.
- [16] Romero E., Vaunat J. (2000) Retention curves of deformable clays. In Tarantino A., Mancuso C. (Eds), *Experimental Evidence and Theoretical Approaches in Unsaturated Soils*, 91–106.
- [17] Cafaro F., Cotecchia F., Cherubini C. (2000) Influence of structure and stress history on the drying behaviour of clays. In Rahardjo, H., Toll, D.G. and Leong, E.C. (Eds), *Unsaturated Soil for Asia*, 633–638.
- [18] Gallipoli D., Wheeler S.J., Karstunen M. (2003) Modeling the variation of degree of saturation in a deformable unsaturated soil. *Géotechnique*, 53:105–112.
- [19] Cafaro F., Cotecchia F. (2015) Influence of the mechanical properties of consolidated clays on their water retention curve. *Rivista Italiana di Geotecnica*, 49:11–27.
- [20] Tamagnini R., Pastor M. (2005) A thermodynamically based model for unsaturated soils: a new framework for generalized plasticity. *Unsaturated Soils - Mancuso & Tarantino (Eds)*, 121–134.
- [21] Fityus S.G., Li J. (2006) Water retention characteristics of unsaturated coal, *Unsaturated Soils 2006*. GSP 147, Fourth International Conference on Unsaturated Soils.
- [22] McCutcheon A., Barton W., Wilson M. (2001) Kinetics of water adsorption/desorption on bituminous coals. *Energy and Fuels*, 15:1387–1395.
- [23] Federico A.M., Miccoli D., Murianni A., Vitone C. (2018) An indirect determination of the specific gravity of soil solids. *Engineering Geology*, 239:22–26.
- [24] Nebel M.L. (1916) Specific gravity studies of Illinois coal. *University of Illinois Bulletin*. Vol XIII, n. 44. Bulletin No. 89 Engineering Experiment Station, Chapman and Hall, Ltd., London.
- [25] Chandler R.J., Gutierrez C.I. (1986) The filter-paper method of suction measurement. *Géotechnique*, 36(2):265–268.
- [26] Chandler R.J., Crilly M.S., Montgomery-Smith G. (1992) A low-cost method of assessing clay desiccation for low-rise buildings. *Proc. Instn. Civ. Engrs*, 2:82–89.
- [27] Terzaghi K. (1923) Die berechnung der durchlassigkeitsziffer des tones aus dem verlauf der hydrodynamischen spannungerscheinungen. *Mathematisch-naturwissenschaftliche Klasse. Akademie der Wissenschaften, Vienna*, 132: 125–138.
- [28] Tadepalli R., Fredlund D.G. (1991) The collapse behavior of a compacted soil during inundation. *Canadian Geotechnical Journal*, 28(4):477–488.
- [29] Sivakumar V., Tan W.C., Murray E.J., McKinley J.D. (2006) Wetting, drying and compression characteristics of compacted clay. *Géotechnique*, 56(1):57–62.
- [30] Li P., Vanapalli S., Li T. (2016) Review of collapse triggering mechanism of collapsible soils due to wetting. *Journal of*

- Rock Mechanics and Geotechnical Engineering, Vol.8 Issue 2, 256–274.
- [31] Zainal A.E., Al-Ebadi L.H. (2016) The effect of varying degree of saturation on settlement rate of collapsible soils. *Applied Research Journal*, 2(1):27–42.
- [32] Qian H.J., Lin Z.G. (1988) Loess and its engineering problems in China. In *Engineering Problems of Regional Soils, Proceedings of the International Conference on Engineering Problems of Regional Soils*, Beijing, China, 136–153.
- [33] Fredlund D.G., Xing A., Huang S. (1994) Predicting the permeability function for unsaturated soils using the soil-water characteristic curve. *Canadian Geotechnical Journal*, 31(4):533–546.
- [34] Leong E.C., Rahardjo H. (1997) Permeability functions for unsaturated soils. *Journal of Geotechnical Engineering, ASCE*, 123:1118–1126.
- [35] Kool J.B., Parker J.C. (1987) Development and evaluation of closed-form expressions for hysteretic soil hydraulic properties. *Water Resources Research*, 23(1):105–114.
- [36] Gribb M.M., Kodesová R., Ordway S.E. (2004) Comparison of soil hydraulic property measurement methods. *Journal of Geotechnical and Geoenvironmental Engineering, ASCE*, 130:1084–1095.
- [37] Bottiglieri O. (2009) Caratterizzazione idraulica di un terreno a grana media parzialmente saturi. PhD thesis, Technical University of Bari, Italy (in Italian).
- [38] Stannard D.I. (1992) Tensiometers: theory, construction and use. *Geotechnical Testing Journal*, 15(1):48–58.
- [39] Šimůnek J., Šejna M., Saito H., Sakai M., van Genuchten M.T. (2013) *The HYDRUS-1D Software Package for Simulating the One-Dimensional Movement of Water, Heat, and Multiple Solutes in Variably-Saturated Media. Version 4.17*, HYDRUS Software Series 3, Department of Environmental Sciences, University of California Riverside, Riverside, California, USA, 343.
- [40] Scott P.S., Farquhar G.J., Kouwen N. (1983) Hysteretic effects on net infiltration. In *Advances in Infiltration*, American Society of Agricultural Engineers Publication 11–83, St. Joseph, Michigan, 11:163–170.
- [41] van Genuchten M.T., Leij F.J., Yates S.R. (1991) *The RETC Code for Quantifying the Hydraulic Functions of Unsaturated Soils, Version 1.0*. EPA Report 600/2-91/065, U.S. Salinity Laboratory, USDA, ARS, Riverside, California.
- [42] Marzulli V., Cafaro F., Ziccarelli M. (2018) Hydraulic characterization of a pervious concrete for deep draining trenches. *Journal of Materials in Civil Engineering*, 30(6):04018100, doi: 10.1061/(ASCE)MT.1943-5533.0002274.
- [43] Lu N., Likos W.J. (2004) *Unsaturated soil mechanics*. John Wiley & Sons, Inc.